

## Transdermal Microneedle Array-based Sensor for Real Time Continuous Glucose Monitoring

Kuo-Yuan Hwa<sup>1,2,\*</sup>, Boopathi Subramani<sup>1</sup>, Po-Wen Chang<sup>3</sup>, Mingnan Chien<sup>4</sup>, Jung-Tang Huang<sup>3,4</sup>

<sup>1</sup>Department of Molecular Science and Engineering, National Taipei University of Technology, Taipei, Taiwan

<sup>2</sup>Center for Biomedical Industry, National Taipei University of Technology, Taipei, Taiwan

<sup>3</sup>Institute of Mechatronic Engineering, National Taipei University of Technology, Taipei, Taiwan

<sup>4</sup>Institute of Mechanical and Electrical Engineering, National Taipei University of Technology, Taipei, Taiwan

\*E-mail: [kyhwa@ntut.edu.tw](mailto:kyhwa@ntut.edu.tw)

Received: 22 November 2014 / Accepted: 31 December 2014 / Published: 19 January 2015

We fabricated a low cost, low power consuming and easy to use continuous glucose monitoring system in this study. The transdermal sensor consists of an electrochemical sensing unit, a signal-processing unit and a power supply unit. The electrochemical sensing unit comprises an array of microneedle. The transdermal sensor is minimally invasive which can pierce the upper layer of the skin. Glucose Oxidase (GOx) was immobilized on the Au microneedle surface by forming self-assembled monolayer with 3-Mercaptopropionic acid (MPA). The GOx immobilized microneedle will be used as a subcutaneous glucose sensor to detect the glucose levels in interstitial fluid (ISF). The cyclic voltammetric studies and the transdermal sensing unit developed in this study were able to detect glucose with linear range of  $30 \text{ mg dL}^{-1}$  to  $400 \text{ mg dL}^{-1}$ . The results showed that the prepared sensor can be used to sense glucose in subcutaneous tissues and are applicable for real-time continuous glucose monitoring system.

**Keywords:** Microneedle, Bluetooth, Continuous Glucose Monitoring System, Interstitial Fluid, Glucose Oxidase

### 1. INTRODUCTION

In recent years, self-monitoring of glucose has seen several major advancements. Capillary blood glucose is predominantly used in diabetic control by patients and healthcare professionals. While advanced techniques have been developed for capillary blood glucose measurements, still this technique is not able to monitor the fluctuating glucose levels due to its limitation in number of tests

per day [1]. These are minimally-invasive finger stick tests which are often painful and a major hindrance to monitor the blood glucose levels on regular basis.

Continuous glucose monitoring system (CGMS) is a useful method in diabetes treatment with advantages over the conventional glucose measurement methods by offering a longer-term ongoing display of glucose levels [2, 3]. However, the CGMS commercially available at present are expensive and there is always a demand exists for cost-effective CGMS. The CGMS consists of an implantable electrochemical biosensor containing a glucose-dependent enzyme immobilized on a microneedle generating glucose-dependent electrical currents. The microneedle will be introduced into subcutaneous tissues and connected to a transmitter and a receiver which displays the glucose profile [4]. Transdermal glucose sensors are usually designed to monitor the change in glucose level continuously for several days. The microneedle tracks blood glucose levels indirectly by measuring the glucose concentration in interstitial fluid of subcutaneous tissues. Numerous therapeutic systems used microneedle based arrays and they have got considerable attention due to their potential application in intradermal sampling and delivery without pain [5, 6]. The microneedle has been used in various sensors including amperometric glucose sensors [7-10]. The microneedle based transdermal biosensors have several advantages over the conventional glucose sensors such as reduced sampling discomfort or pain, which increases the user's willingness to use and less intrusive under the continuous monitoring of glucose, besides reducing skin damage and wound infections can be avoided. The microneedle was used only for withdrawing analyte from ISF through capillary action in these sensors and they were not used as sensors. As the microneedle will be in contact with skin surface for few days, highly biocompatible materials have to be used to avoid any adverse reaction of the material with the skin. Therefore the microneedle made of materials such as steel, nickel, nickel alloy, carbon nanotubes, or silicon can be selected and their surface may be covered with biocompatible metals such as gold, palladium, nickel alloy.

In the last two decades, a wide range of possible implantable glucose biosensors based on different materials and membranes have been developed [1]. An ideal biosensor will be the one, which monitors blood glucose variations in real time throughout the day and over prolonged time under harsh conditions. The sensor must be of very small size and appropriate for easy implantation with little discomfort [11]. The immobilization of enzyme on the electrode surface is an important step in defining the performance of a biosensor. The covalent binding of enzymes on a modified electrode surface through self-assembled monolayers (SAM) has received considerable interest in this regard [12]. SAMs are very useful in developing nano-scale biosensor because they are easy to prepare on a metallic structure with various functional groups, which can be linked to macromolecules such as enzymes. The SAMs formed on gold surface are widely used for enzyme immobilization in biosensor applications [5]. The SAMs acts as a shield for the enzymes on the electrode surface and prevent them from denaturation [8]. This property is particularly useful in fabricating biosensors for CGMS.

We developed a subcutaneous glucose sensing system by immobilizing glucose oxidase enzyme on the microneedle surface and used Bluetooth low energy technology to transfer the signals to PC. The glucose oxidase GOx was immobilized on the Au microneedle surface by forming self-assembled monolayers (SAM) to detect the glucose in ISF.

## 2. MATERIALS AND METHODS

### 2.1 Materials

Glucose Oxidase (GOx) (type x-s from *Aspergillus niger*), 3-Mercaptopropionic acid (MPA), N-(3-Dimethylamino-propyl)-N'-ethylcarbodiimide hydrochloride (EDC), N-Hydroxysuccinimide (NHS), Polyallylamine were purchased from Sigma-Aldrich and used as received. All other reagents used were of analytical grade. Au microneedle was purchased from Formosa Taffeta Company, Taiwan. Bluetooth 4.0 transmitter and dongle was obtained from Texas Instruments, Taiwan. AD8500 amplifier was purchased from Analog Devices, Taiwan. The supporting electrolyte 50 mM phosphate buffer solution (PBS) was prepared from Na<sub>2</sub>HPO<sub>4</sub> and NaH<sub>2</sub>PO<sub>4</sub>.

### 2.2 Apparatus

The electrochemical measurements were carried out using CHI 1211B handheld potentiostat. Electrochemical studies were carried out in a conventional three electrode cell using Au electrode and Au microneedle (CHI) as working electrodes (area 0.07 cm<sup>2</sup>), saturated Ag/AgCl and Ag microneedle as reference electrodes and Pt wire and uncoated Au microneedle as counter electrodes. EIM6ex ZAHNER (Kroanch, Germany) was used for electrochemical impedance spectroscopy (EIS) studies.

### 2.3 Immobilization of GOx on modified Au electrode and microneedle

The Au electrode surface was cleaned by electrochemical oxidation/reduction in 0.05 M H<sub>2</sub>SO<sub>4</sub> for 30 min from +1.5 to -0.3 V vs Ag/AgCl at 0.1 V s<sup>-1</sup>. The electrode was then washed with water and ethanol. The Au electrode with enzyme-containing matrix was prepared with the following methods [13]. The layer of MPA on the Au electrode was prepared by immersing in an ethanol solution containing 1 mM MPA for 1 h. Au/MPA electrode was then modified by EDC-NHS to activate the carboxyl group, and used to immobilize GOx. 2 mM EDC and 5 mM NHS was drop casted on the electrode and kept for 50 min to activate the carboxyl group. Then the electrodes were washed thoroughly with PBS. 10 µL of GOx in PBS at 5 mg/mL conc. was drop casted on the electrode and kept at 4°C for 2 hours.

Electrochemical Impedance Spectroscopy (EIS) measurements were performed in PBS containing 5 mM Fe(CN)<sub>6</sub><sup>3-/4-</sup> in the frequency range of 100 mHz for various modified electrodes with and without GOx. The Randles' equivalent circuit model was used for explaining the EIS experimental data. The circuit included the Warburg element to consider the diffusion controlled process at low frequency region. Nyquist plot was drawn with Imaginary resistance versus real resistance. The Au microneedle surface was cleaned by a two-step process by using potassium hydroxide and hydrogen peroxide as explained by [14]. Briefly, the microneedle was soaked in 50 mM KOH and 25% H<sub>2</sub>O<sub>2</sub> and rinsed with double distilled water. Then it was placed in 50 mM KOH solution and electrochemically swept from 200 to 1200 mV against Ag/AgCl electrode at 50 mV s<sup>-1</sup>. The surface cleaned microneedle was then washed with water and ethanol. The microneedle with

enzyme containing matrix was prepared by following the same method described above for the Au electrode.

#### 2.4 Assembly of subcutaneous sensor

Fig. 1 shows the simplified scheme of the electrochemical sensor circuit used in this study. Electrochemical sensors work by allowing the analyte present in ISF to interact with the working electrode (WE) microneedle immobilized with GOx. The reference electrode (RE) Ag microneedle provides feedback to maintain a constant potential with the WE terminal by varying the voltage at the bare Au microneedle, which act as a counter electrode (CE). The direction of the current at the WE terminal depends on whether the reaction occurring is oxidation or reduction. In case of glucose catalysis, oxygen reduction takes place, therefore the current flows into the working electrode, which requires the counter electrode to be at a negative voltage (typically 300 mV to 400 mV) with respect to the working electrode.

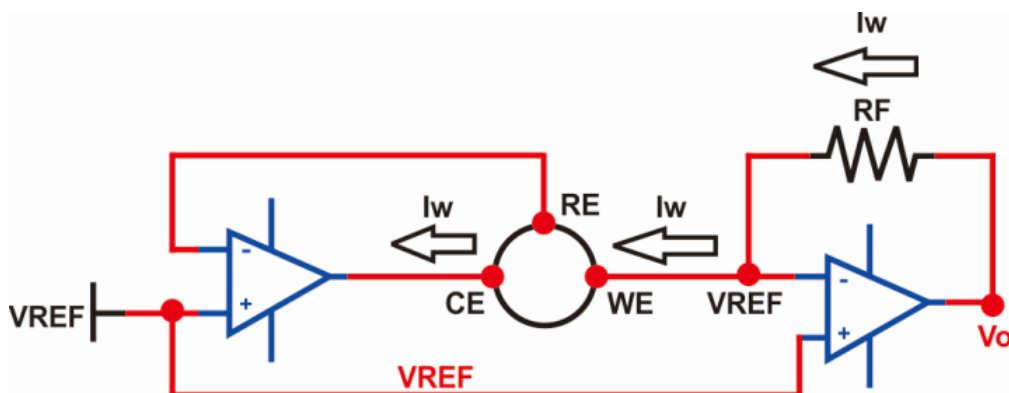


**Figure 1.** Schematic diagram of simplified electrochemical sensor circuit.

The current flowing into WE terminal is less than 100 nA for each mg dL<sup>-1</sup> concentration, therefore, converting this current into an output voltage requires a transimpedance amplifier with a very low input bias current. The AD8500 Operational Amplifier (Op Amp) has CMOS inputs with maximum input bias current of 1 pA at room temperature, making this Op Amp appropriate for our application. The 2.5 V, LM385 establishes pseudo-ground reference for the circuit, which allows for single-supply operation while consuming very little quiescent current. The amplifier sinks enough current from the CE terminal to maintain a 0 V potential between the WE and RE terminals on the sensor. The RE terminal is connected to the inverting input, therefore no current flows in or out of it. This means that the current comes from the WE terminal, and it changes linearly with the glucose concentration present in ISF. Transimpedance Amplifier converts the sensor current into a voltage proportional to glucose concentration. The complete setup of the subcutaneous sensor is shown in Fig. 2. The setup consists of an array of microneedles attached to the bottom of a base plate and on the top of the base plate Bluetooth 4.0, battery and transmitter were present (Fig 2a and 2b). The Bluetooth module BT4.0s used for data transfer with the size of 25 mm x 13 mm as shown in Fig. 2c. Its main

function is for wireless data transmission, to get rid of unwanted parts, and its top has done an accelerometer pin, users to use, simply solder the chip. The Bluetooth USB (Fig. 2d) dongle connected to a PC receives the signal from the transmitter and transfers it to PC.

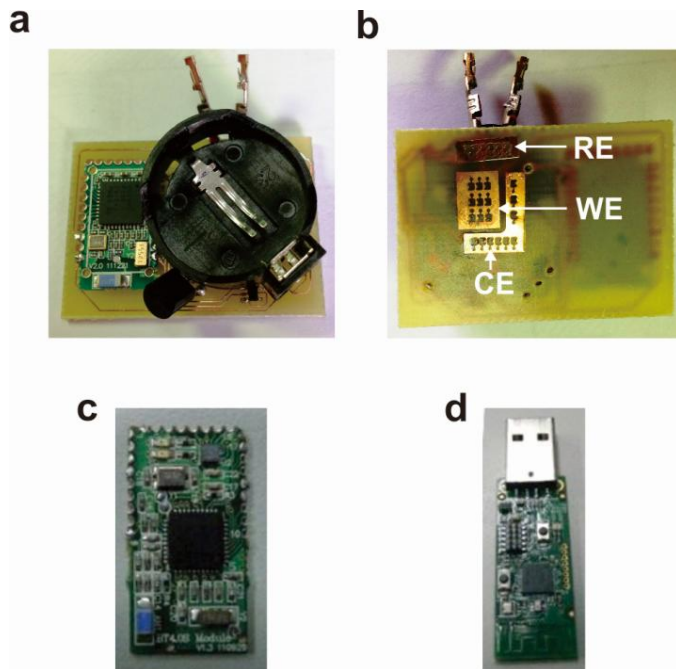


**Figure 2.** Transdermal Micro needle Array-based Sensor for Real time Continuous Glucose Monitoring System. a. Battery and the transmitter are attached to the top of the base plate. b. Microneedle consists of GOx coated Au microneedle as working electrode (WE), Ag microneedle as reference electrode (RE) and bare Au microneedle as counter electrode (CE). c. BT4.0 module circuit board physical map. d. CC2540 USB Dongle.

### 3. RESULTS AND DISCUSSION

#### 3.1 EIS of SAM modified Au electrode

EIS was used to study the GOx immobilized on the SAM modified Au electrode surface [15]. The complex plane plots obtained for bare Au, SAM modified Au electrodes with and without GOx are given in Fig. 3. The bare Au electrode exhibited an almost straight line, which is a characteristic feature of diffusion limited electrochemical process. The electrode surface with SAM formed an insulating layer which acts as a barrier to the interfacial electron transfer. This was observed by the appearance of the small semicircular part of the spectrum. The size of the respective semicircular element corresponds to the electron-transfer resistance ( $R_{et}$ ) at the electrode surface. As shown in Fig. 3, an increase in semicircular diameter of the impedance spectrum was observed when incubating the Au-SAM modified electrode with GOx indicates formation of a ferrocyanide transport-blocking layer on the electrode. This indicates that SAM formed by MPA on the Au electrode surface act as a large barrier to electron transfer occurs at the GOx modified Au electrode rather than bare Au electrode.

This was revealed by the increase in diameter of the semicircle in EIS spectrum. The increased electron transfer resistance observed at GOx modified Au electrode could be due to the thick protein layer surrounding the FAD redox center of GOx [1]. The EIS results are consistent with the CV experiment which demonstrates that GOx was well immobilized at the Au/MPA modified electrode.

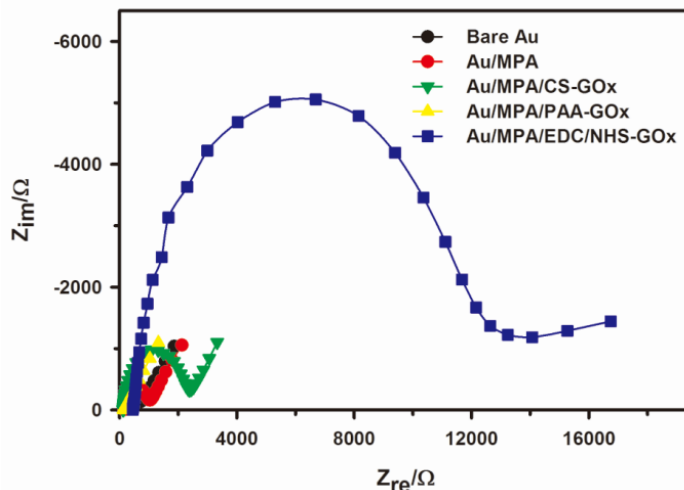
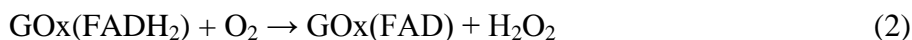


**Figure 3.** EIS of GOx immobilized on MPA modified Au electrode.

The higher density of GOx enzyme on the gold surface is determined by the arrangement of sulfuric group and proximity between the metal atoms. Moreover, the high degree of van-der Waals interactions with nearby molecules mainly defines the macroscopic properties of the SAMs. In addition, the linkage of GOx will be affected by the overall macroscopic properties. It has been reported that the amine group present in the GOx couples with the acidic group of Au/MPA SAM, by forming imide group with the help of EDC and NHS [15]. So the Au-MPA surface with its carboxyl group activated by EDC/NHS can be a good matrix support suitable for fabricating implantable glucose sensor devices.

### 3.2 Electrochemical detection of glucose by Au/MPA/GOx electrode

The first-generation glucose sensors used flavoenzyme glucose oxidase (GOx) immobilized on a working electrode. The redox cofactor of GOx flavin adenine dinucleotide (FAD) catalyzes the oxidation of glucose to glucanolactone, as shown in equations (1) and (2) [16].



The  $\text{H}_2\text{O}_2$  produced from the above reaction is measured by electrochemically on the surface of the working electrode via equation (3), which relates current to glucose concentrations obtained from a calibration plot.



The second generation biosensors employed redox mediators to decrease the oxygen dependence for the catalysis of glucose whereas the third generation, the GOx is covalently linked to the electrode surface through its redox cofactor [1]. First-generation glucose sensors are preferred over second and third generation sensors for implantable biosensors, as the later two have not been tested *in vivo* [17].

We investigated the electrochemical properties of the Au/MPA/GOx modified electrode with a conventional three-electrode cell connected to the potentiostat/galvanostat. Fig. 4 shows the CV of modified electrodes with GOx in oxygen saturated PBS at  $0.05 \text{ V s}^{-1}$  scan rate with various concentrations of glucose. The cyclic voltammetry results showed that the MPA modified electrodes showed higher electrocatalytic activity for glucose in the presence of oxygen. Thus, glucose was effectively oxidized at the composite film. This electrocatalytic response towards glucose was higher with MPA/GOx than that was observed in MPA/CS/GOx and MPA/PAA/GOx (data not shown). This showed the efficient electrocatalytic ability of the SAM modified electrodes towards glucose oxidation as concomitant redox peaks were observed for the increased glucose concentration from 1-14 mM of glucose. The linear range of glucose detection is about  $0 \text{ mg dL}^{-1}$  to  $250 \text{ mg dL}^{-1}$  in the presence of oxygen (Fig. 4 inset). There are reports about direct electrochemical behavior of GOx on modified glassy carbon electrodes, but there was no direct electrochemistry observed for GOx on Au electrodes in oxygenated PBS.

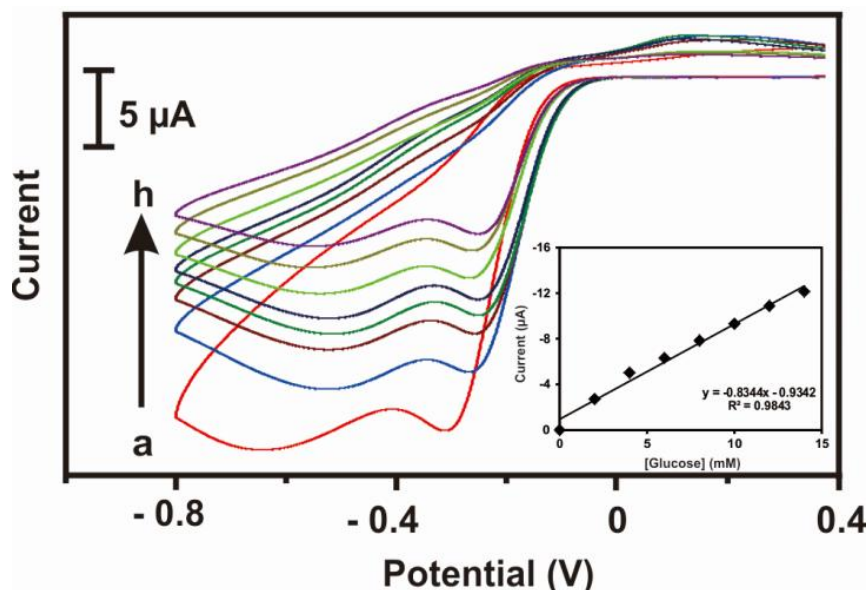


**Figure 4.** Cyclic voltammetry of Au/MPA/GOx electrode with 0-14 mM glucose (*a* to *h*) in oxygenated PBS. Inset: Linear plot of [glucose] (0 to 14 mM) vs. peak current.

### 3.3 Electrocatalytic determination of glucose by Au/MPA/GOx microneedle

The Au/MPA/GOx microneedle was tested for electrocatalysis of glucose in oxygen saturated PBS, pH 7.0. Fig. 5 shows the cyclic voltammetry studies of modified Au microneedle in oxygenated PBS in the absence of glucose (curve a), exhibited a large cathodic peak appeared at around  $-0.25$  V ascribed to the reduction of oxygen. When 100 mg dL $^{-1}$  concentration of glucose was added to the electrolyte solution, the reduction peak current decreased. Moreover, the cathodic peak current decreased linearly with increase in glucose concentration over the linear range of 30 mg dL $^{-1}$  to 400 mg dL $^{-1}$ . The decrease in oxygen concentration upon addition of glucose can be explained by the equations: (1-3) [18]. A calibration plot between concentration of glucose and their respective peak currents gave a linear plot (Fig. 4 inset,  $R^2 > 0.991$ ). The excellent analytical parameters revealed the capability of the sensor towards determination of glucose via reductive detection of oxygen.

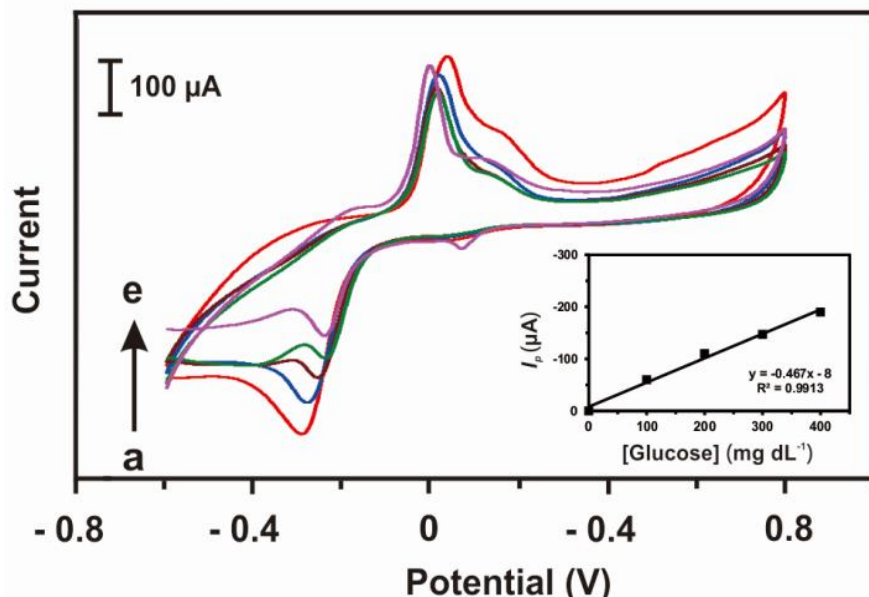


**Figure 5.** Cyclic voltammetry of GOx immobilized microneedle in glucose concentration ranging from 0 mg dL $^{-1}$  – 400 mg dL $^{-1}$ . Inset: Linear plot of [glucose] (100 to 400 mg/dL) vs. peak current.

### 3.4 Electronic circuit and data analysis

The output voltage of the transimpedance amplifier was

$$V_o = 0.7 V + I_{WE} \times R_F \quad (4)$$

where  $I_{WE}$  is the current flowing into the WE terminal, and  $RF$  is the transimpedance feedback resistor.

The maximum response of the sensor was 58.8 nA $^{-1}$  mg dL $^{-1}$  for glucose, and its maximum input range was 400 mg dL $^{-1}$  of glucose solution. So the maximum output current was 23.5  $\mu$ A, and the maximum output voltage was determined by the transimpedance resistor, as shown in equation 5.

$$\begin{aligned} V_o &= 0.7 V + 400 \text{ mg dL}^{-1} \times 58.8 \text{ nA}^{-1} \text{ mg dL}^{-1} \times R_F \\ V_o &= 0.7 V + 23.5 \mu\text{A} \times R_F \end{aligned} \quad (5)$$

Operating the circuit with 3 V supply resulted in a usable range of 0.7 V ~ 3 V at the output of transimpedance amplifier. We selected a 100 K $\Omega$  resistor for the transimpedance feedback resistor which gives a maximum output voltage of 3 V and it allows for approximately 8% over range.

Resistor R4 keeps the noise gain at a reasonable level. Selecting the value of this resistor is a compromise between the magnitude of the noise gain and the sensor settling time errors when exposed to high concentrations of glucose. For example, if, R4 = 33  $\Omega$ , it can result in a noise gain of 349, as shown in Equation 6.

$$NG = 1 + 100 k\Omega (R_F) / 330\Omega = 304 \quad (6)$$

The input noise of the transimpedance amplifier appeared at the output amplified by the noise gain. For this circuit, we were only interested in low frequency noise as the sensor is only operated at low frequency. The AD8500 had a 0.1 Hz to 10 Hz input voltage noise of 6  $\mu V_{p-p}$ , therefore the noise at the output was 1.82  $mV_{p-p}$ , as shown in Equation 7.

$$V_{Output\ noise} = 6 \mu V \times NG = 1.82 mV_{p-p} \quad (7)$$

As this was very low frequency 1/f noise, it was very hard to filter out. However, the sensor response was also very slow; therefore, we could take advantage of this by using a very low frequency low-pass filter (R5 and C6) with a cutoff frequency of 0.16 Hz. Even with such a low frequency filter, its effect on the sensor response time is negligible when compared to the 30 s response time of the sensor.

One of the important characteristic of electrochemical sensors are their longevity. When it was first powered up, it took several minutes for the output signal to settle to its final value. When exposed to a higher concentration of the glucose, the time required for the sensor output to reach 90% of its final value was in the order of 25 s to 30 s. The reason for delayed response is if the voltage between the RE and WE terminals had a sudden change in magnitude, it will take several minutes for the sensor's output current to settle down. This also applies when cycling power to the sensor. To avoid very long startup times, P-channel JFET Q1 shorts the RE terminal to the WE terminal when the supply voltage drops below the JFET's gate-to-source threshold voltage (~2.5 V). Two AAA batteries or a 3 V power supply powers the circuit. Q2 provides reverse voltage protection, and the AD8500 regulates the input supply to the 3 V required to power the sensor.

### *3.5 In vitro testing of the microsensor*

The size of the microneedle used for the sensor determines the level of pain encountered by patients. Currently, the pinhead size of microneedle available on the market is either 0.51 mm or 0.71 mm. When using these types of needles for glucose determination can be painful due to the deep penetration of the needle into the subcutaneous tissues. Studies have shown that smaller the size of microneedle's pinhead lesser the pain. With the satisfaction of patients in mind, we used a microneedle array with a reduced pinhead size in this study.

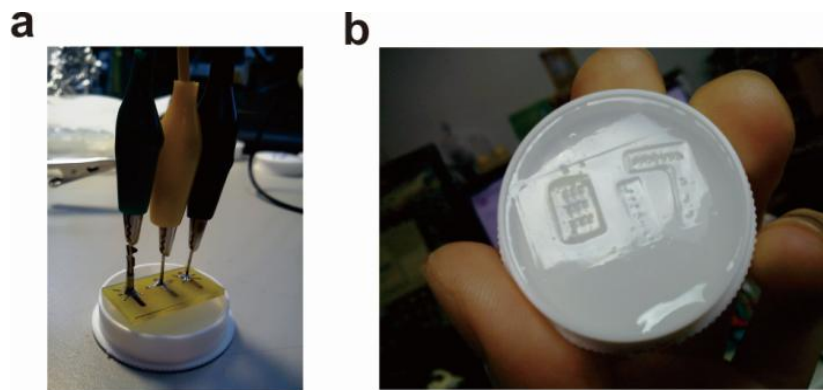


**Figure 6.** The three electrode system consisting of working electrode, reference electrode and counter electrode on 1% agarose gel.

We tested the GOx immobilized microneedle sensor in 1% agarose gel (Fig. 6). The gels were prepared with different concentrations of glucose and current response was measured at 0.7 V. A linear response was observed with increasing glucose concentrations ranging from  $50 \text{ mg dL}^{-1}$  to  $400 \text{ mg dL}^{-1}$  (Fig. 7,  $R^2 > 0.998$ ).  $500 \text{ mg dL}^{-1}$  gave very high signal and it was outside the range of the converter. Thus the GOx coated Au microneedle sensor was able to sense glucose in the physiological range. The durability of the GOx immobilized microneedle was checked for 7 days. The results showed that enzyme retained more than 80% activity after 7 days (data not shown), which is essential for CGMS. This demonstrated the feasibility of our method for quantitative measurement of glucose in ISF.

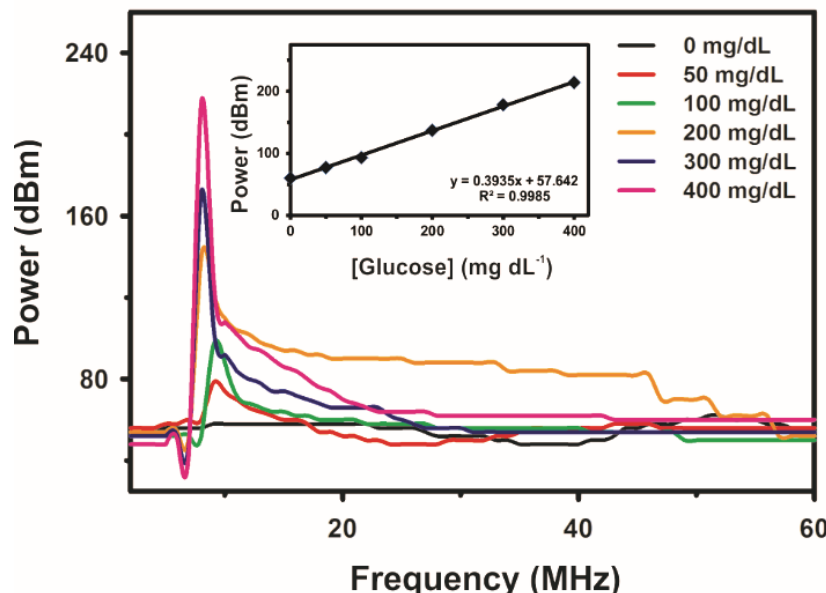


**Figure 7.** Determination of glucose by real-time glucose monitoring system. The signal from the converter shows output power increases with response to glucose concentration ranging from  $0 \text{ mg dL}^{-1}$  –  $400 \text{ mg dL}^{-1}$ .

#### 4. CONCLUSION

The concept of transcutaneous microneedle array that accomplish the continuous monitoring of glucose in diabetic patients is an attractive solution to keep the disease under control. The development of implantable glucose sensors for continuous glucose monitoring has to overcome several challenges including the long-term stability of the enzyme, oxygen deficiency, tissue inflammatory response, calibration, etc., The stability of the enzyme on the electrode surface can be enhanced by the SAM modified Au surface. Bluetooth 4.0 transmission technology was used in our transdermal glucose sensors. Our sensor consumed less power than other reported Bluetooth sensing modules and, can last at least 10 working hours. This long duration of power is the direction towards uninterrupted monitoring of glucose. Further experiments will be performed in animal models and clinical trials to check the compatibility of the sensor. The future direction of the work will be towards increasing the stability of GOx on the Au microneedle surface by forming a hydrogel or layer by layer assembly with the help of suitable polymers.

#### ACKNOWLEDGEMENT

This study was supported by the grants from National Taipei University of Technology, NTUT-100-140-05 and NTUT-101-140-2-53 to J.T. Huang and K.-Y. Hwa.

#### References

1. J. Wang, *Chem. Rev.*, 108 (2008) 814.
2. M.M. Ahmadi, G.A. Jullien, *IEEE T. Biomed. Circ. S.*, 3 (2009) 169.
3. R.A. Croce, S. Vaddiraju, F. Papadimitrakopoulos, F.C. Jain, *Sensors*, 12 (2012) 13402.
4. A. El-Laboudi, N.S. Oliver, A. Cass, D. Johnston, *Diabetes Technol. The.*, 15 (2013) 101.
5. S.H. Bariya, M.C. Gohel, T.A. Mehta, O.P. Sharma, *J. Pharm. Pharmacol.*, 64 (2012) 11.
6. S. Swain, S. Beg, A. Singh, C.N. Patro, M.E.B. Rao, *Curr. Drug Deliv.*, 8 (2011) 456.
7. S.-O. Choi, Y. Kim, J.-H. Park, J. Hutcheson, H. Gill, Y.-K. Yoon, M.R. Prausnitz, M.G. Allen, *Biomed Microdevices*, 12 (2010) 263.
8. J.C. Harper, S.M. Brozik, J.H. Flemming, J.L. McClain, R. Polsky, D. Raj, G.A. Ten Eyck, D.R. Wheeler, K.E. Achyuthan, *ACS Appl. Mater. Interfaces*, 1 (2009) 1591.
9. P.R. Miller, S.A. Skoog, T.L. Edwards, D.M. Lopez, D.R. Wheeler, D.C. Arango, X. Xiaoyin, M. B. Susan, J. Wang, R. Polsky, Roger J. Narayan, *Talanta*, 88 (2012) 739.
10. J.R. Windmiller, N. Zhou, M.-C. Chuang, G. Valdes-Ramirez, P. Santhosh, P.R. Miller, R. Narayan, J. Wang, *Analyst*, 136 (2011) 1846.
11. B. Feldman, R. Brazg, S. Schwartz, R. Weinstein, *Diabetes Technol. The.*, 5 (2003) 69.
12. S. Garg, H. Zisser, S. Schwartz, T. Bailey, R. Kaplan, S. Ellis, L. Jovanovic, *Diabetes Care*, 2006 (9) 44.
13. T.M. Nahir, E.F. Bowden, *Electrochim. Acta*, 39 (1994) 2347.
14. L.M. Fischer, M. Tenje, A.R. Heiskanen, N. Masuda, J. Castillo, A. Bentien, J. Émneus, H.J. Mogens, A. Boisen, *Microelect. Engg.*, 2009 (86) 1282.
15. J.V. Staros, R.W. Wright, D.M. Swingle, *Anal. Biochem.*, 1986;156:220-2.
16. S. Vaddiraju, I. Tomazos, D.J. Burgess, F.C. Jain, F. Papadimitrakopoulos, *Biosens. Bioelectron.*, 2010 (25) 1553.

17. F. Mizutani, Y. Sato, S. Yabuki, T. Sawaguchi, S. Iijima, *Electrochim. Acta*, 1999 (44) 3833.
18. K. Manesh, H.T. Kim, P. Santhosh, A. Gopalan, K.-P. Lee, *Biosens Bioelectron.* 2008 (23) 771.

© 2015 The Authors. Published by ESG ([www.electrochemsci.org](http://www.electrochemsci.org)). This article is an open access article distributed under the terms and conditions of the Creative Commons Attribution license (<http://creativecommons.org/licenses/by/4.0/>).